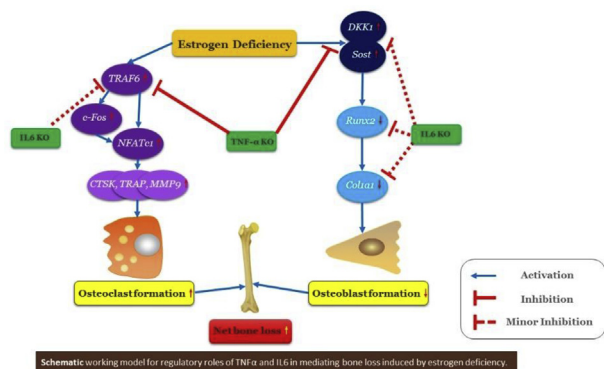


effect in inhibiting bone formation and enhancing TRAF6 mediated osteoclastogenesis than IL6, suggesting the role of different regulatory mechanisms governing TNF $\alpha$  and IL6 action on bone metabolism.



## Bone Biology

### 154 PROTEOMIC ANALYSIS OF OSTEOBLASTS SECRETOME PROVIDES NEW INSIGHTS IN MECHANISMS UNDERLYING OSTEOARTHRITIS SUBCHONDRAL BONE SCLEROSIS

C. Sanchez, G. Mazzucchelli, C. Lambert, F. Comblain, E. DePauw, Y. Henrotin. Univ. of Liège, Liège, Belgium

**Purpose:** Osteoarthritis (OA) is characterized by cartilage degradation but also by other joint tissues modifications like subchondral bone sclerosis. In this study, we used a proteomic approach to compare secretome of osteoblast isolated from sclerotic (SC) or non sclerotic (NSC) area of OA subchondral bone.

**Methods:** Secretome was analyzed using differential quantitative and relative label free analysis on nanoUPLC G2 HDMS system. mRNA of the more differentially secreted proteins were then quantified by RT-PCR and the most relevant proteins identified using western-blotting and immunoassays.

**Results:** 175 proteins were identified in NSC osteoblast secretome. Compared to NSC osteoblast secretome, 13 proteins were significantly less secreted (Osteomodulin, CSF-1, IGFBP5, VCAM-1, IGF2, 78 kDa glucose-regulated protein, versican, calumenin, IGFBP2, thrombospondin-4, periostin, reticulocalbin 1 and osteonectin), and 12 proteins were significantly more secreted by SC osteoblasts (CHI3L1, fibulin-3, SERPINE2, IGFBP6, SH3BGR13, SERPINE1, reticulocalbin3, alpha-2-HS-glycoprotein, TIMP-2, IGFBP3, TIMP-1, SERPINF1). Similar changes in periostin, osteomodulin, SERPINE1, IGFBP6, fibulin-3 and CHI3L1 mRNA levels were observed. Finally, osteomodulin and fibulin-3 specific sequences were quantified by western blot and immunoassays in serum and culture supernatants.

**Conclusions:** We highlighted some proteins differentially secreted by the osteoblasts coming from OA subchondral bone sclerosis. These changes contribute to explain some features observed in OA subchondral bone, like the increase of bone remodeling or abnormalities in bone matrix mineralization. Among identified proteins, osteomodulin was found decreased and and fibulin-3 increased in serum of OA patients. These findings suggest that osteomodulin and fibulin-3 fragments could be biomarkers to monitor early changes in subchondral bone metabolism in OA.

### 155 EFFECT OF DENOSUMAB ON BONE FORMATION MARKER P1NP

H. Tanigawa<sup>†‡</sup>, T. Maeda<sup>†</sup>, K. Kumagai<sup>†</sup>, S. Imai<sup>†</sup>. <sup>†</sup>Shiga Univ. of Med. Sci., Otsu, Japan; <sup>‡</sup>Kusatsu Gen. Hosp., Kusatsu-city, Shiga, Japan

**Purpose:** Type I procollagen N-terminal propeptide (PINP) is considered the most sensitive bone formation marker and it is useful for monitoring osteoporosis treatment such as bone formation or anti-resorptive therapy. In our hospital, we have administered Denosumab, an anti-RANKL antibody as a treatment for osteoporosis. In addition to bone mineral determination (DXA method), P1NP and serum NTx are used as osteogenic markers and bone resorption markers, respectively, for its therapeutic effect determination. In past reports it has been reported that there are many cases in which P1NP falls below the

standard lower limit (17.1  $\mu\text{g/L}$ ) in patients using bisphosphonate (BP). The purpose of this study was to investigate the state of P1NP value in cases treated with denosumab.

**Methods:** For January 2015 - December 2016, we evaluated P1NP and NTx for 30 patients with osteoporosis who administered denosumab at our hospital. For each marker, the percentage of cases below the baseline lower limit was compared.

**Results:** Denosumab administration resulted in P1NP below the reference lower limit value in 15 cases (50%). In NTx, there were no cases below the reference lower limit. There were no cases of apparent atypical femoral fractures during the follow-up period. In 24 patients who were able to measure P1NP from the first dose of denosumab, the transition of the P1NP value was observed. All cases were within the reference values before the initial prescription, but 11 cases (46%) were lower than the reference lower limit value during administration of denosumab for an average of 6 months.

**Conclusions:** Denosumab strongly suppresses bone turnover and also decreases bone metabolism markers. When both the bone formation marker and the bone resorption marker are below the lower limit value, it is serologically in the state of inhibition of excessive bone turnover (SSBT) and may contribute to atypical fracture (Kitaori et al., 2004). In this study, P1NP was lower than the lower limit in half cases in patients treated with denosumab, but it is difficult to think of all these cases as SSBT status. There are reports that there are cases in which P1NP is below the lower limit in certain proportions even in BP administered patients (Eastell et al., 2011). It is difficult to use P1NP as a hazard marker of SSBT in patients receiving bone resorption inhibitors including denosumab. It may be necessary to set new reference values for P1NP for cases using bone resorption inhibitors. In patients using denosumab, P1NP fell below the reference lower limit in 50%. In patients with bone resorption inhibitors including denosumab, it may be necessary to examine new reference values for P1NP.

### 156 GENERATION AND PHENOTYPING OF A TARGETED MOUSE MODEL OF ALKAPTONURIA

J.H. Hughes<sup>†</sup>, K. Liu<sup>†</sup>, H. Sutherland<sup>†</sup>, P.J. Wilson<sup>†</sup>, A.T. Hughes<sup>†‡</sup>, A.M. Milan<sup>†‡</sup>, L.R. Ranganath<sup>†‡</sup>, J.A. Gallagher<sup>†</sup>, G. Bou-Gharios<sup>†</sup>. <sup>†</sup>Univ. of Liverpool, Liverpool, United Kingdom; <sup>‡</sup>Royal Liverpool and Broadgreen Univ. Hosp. NHS Trust, Liverpool, United Kingdom

**Purpose:** Alkaptonuria (AKU) is a rare autosomal recessive metabolic disease caused by mutations in the gene homogentisate 1,2-dioxygenase (HGD). Deficiency of HGD leads to an accumulation of homogentisic acid in the blood and tissues. Overtime, HGA is polymerised to form a pigment which deposits into connective tissues, particularly in cartilage. The cartilage becomes brittle and osteoarthropathy manifests in early adulthood, becoming very debilitating as it progresses. Studying rare diseases with extreme phenotypes like AKU aid our understanding about more common disorders like osteoarthritis. The current mouse model for AKU was generated by chemical mutagenesis. To overcome the uncertainty of this model harbouring other potentially confounding uncharacterised mutations, we generated a specific HGD (Homogentisate 1,2-dioxygenase) null mouse with the advantage of conditional deletion.

**Methods:** Embryonic stem cells in the C57BL6 background with disrupted HGD gene function were obtained from the Knockout Mouse Project (KOMP). This knockout first plasmid contains the insertion of an IRES:lacZ trapping cassette and a promoter-driven neo cassette into the fifth intron of the HGD gene with the sixth exon flanked by LoxP sequences (HGD tm1a). FLP recombinase reverts the mutation back to wildtype with a floxed critical exon (HGD tm1c). The model then becomes conditional though Cre recombinase which removes the floxed exon resulting in a mutant transcript (HGD tm1d). The Hgd tm1a knock-out first model is characterised here.

**Results:** Homozygous tm1a mice show black urine stained cage bedding, one of the first AKU symptoms. Homogentisic acid is elevated in the homozygous tm1a in both the urine (99,575  $\mu\text{mol/L}$ ) and plasma (100.5  $\mu\text{mol/L}$ ) compared to C57BL6 wildtype mice (urine; 0.9  $\mu\text{mol/L}$ , plasma; 1.7  $\mu\text{mol/L}$ ). Heterozygous tm1a and tm1c mice have levels of HGA comparable to the C57BL6 wildtype. Ochronosis, pigmentation of chondrocytes found within calcified articular cartilage, was detected at 9 weeks in the tm1a mouse as pericellular pigmentation. At 26 and 40 weeks, numerous fully pigmented chondrocytes can be seen in the homozygous tm1a knee cartilage with no evidence of ochronosis in

heterozygous mice. The  $\beta$ -galactosidase transgene (LacZ) that is knocked in to the *tm1a* mouse to disrupt gene function was used to localise HGD expression. Whole-mount staining of several adult tissues from *tm1a* mice shows positive expression in the liver and kidney cortex but no other organs in development nor in adult mice.  $\beta$ -galactosidase staining demonstrates transgene activity throughout the parenchymal cells and is confined to the proximal convoluted tubule cells of the kidney cortex.

**Conclusions:** This novel conditional HGD null mouse exhibits all the main symptoms of AKU. There is no evidence of haploinsufficiency. The knock in LacZ transgene was successfully used to localise HGD expression.

## 157

### 3D ANALYSIS OF LOCAL GREY-LEVEL VARIANCE FROM MICRO-CT IMAGES IS ASSOCIATED WITH OSTEOCYTE CELLULARITY IN HUMAN OSTEOARTHRITIC SUBCHONDRAL BONE

S.S. Karhula<sup>†</sup>, M.A. Finnilä<sup>†,‡</sup>, D.M. Cooper<sup>§</sup>, D. Miller<sup>||</sup>, M. Valkealahti<sup>¶</sup>, A. Joukainen<sup>#</sup>, P. Lehenkari<sup>†</sup>, H. Kröger<sup>#</sup>, R.K. Korhonen<sup>‡</sup>, H.J. Nieminen<sup>†,‡</sup>, S. Saarakkala<sup>†</sup>. <sup>†</sup>Univ. of Oulu, Oulu, Finland; <sup>‡</sup>Univ. of Eastern Finland, Kuopio, Finland; <sup>§</sup>Univ. of Saskatchewan, Saskatoon, SK, Canada; <sup>||</sup>Canadian Light Source Inc., Saskatoon, SK, Canada; <sup>¶</sup>Oulu Univ. Hosp., Oulu, Finland; <sup>#</sup>Kuopio Univ. Hosp., Kuopio, Finland; <sup>††</sup>Aalto Univ., Espoo, Finland

**Purpose:** Subchondral bone remodeling increases in osteoarthritis (OA) causing alterations in bone mineralization at the tissue level as well as changes in osteocyte morphology. Quantification of morphological features of osteocytes in 3D usually requires synchrotron-based micro-computed tomography (SR $\mu$ CT). Quantifying these features with conventional desktop  $\mu$ CT systems requires extremely small samples to provide sufficient resolution ( $>1\mu\text{m}$ ) and thus cell segmentation and analysis from representative human osteochondral cores is challenging. On the other hand, tissue mineral density (TMD) can be readily determined using calibration phantoms with desktop  $\mu$ CT systems. In principle, texture based analysis methods with desktop  $\mu$ CT systems, such as grey-level co-occurrence matrix analysis (GLCM), could provide quantifiable features directly associated to osteocyte cellularity and/or TMD. In this study, we tested this hypothesis by calculating the local variance of 3D GLCM from desktop  $\mu$ CT data and compared the results with reference data from SR $\mu$ CT and TMD calibration.

**Methods:** A total of 26 cylindrical osteochondral cores ( $\varnothing=4\text{mm}$ ) were drilled from the tibial plateau and femoral condyles from 7 total knee arthroplasty patients (approval no 78/2013, Ethical Committee of the Northern Ostrobothnia Hospital District, Finland) and from 2 cadavers (approval no 58/2013 & 134/2015, Research Ethics Committee of the Northern Savo Hospital District, Finland). The samples were first imaged with a desktop  $\mu$ CT system (Skyscan 1272, Bruker microCT, Kontich, Belgium, parameters: 50kV, 200 $\mu\text{A}$ , 2.75 $\mu\text{m}$  pixel size, 1200 projections from 360°, and with 0.5mm Al filter). Subsequently, the same samples were imaged with SR $\mu$ CT at the Canadian Light Source (Saskatoon, SK, Canada) on the BMIT-ID (05ID-2) beamline (parameters: 31keV, 0.9 $\mu\text{m}$  pixel size, and 720 projections from 180°) to determine the osteocyte cellularity in subchondral bone. To evaluate OA severity, conventional histology with safranin O staining was performed, and the histological sections were graded with OARSI grading system. SR $\mu$ CT and  $\mu$ CT datasets were co-registered and a volume-of-interest of 1980x1980x2000 $\mu\text{m}^3$  was selected. Prior to analysis, a bone mask (excluding the trabecular holes and vessel cavities) was generated from  $\mu$ CT data and applied to both the SR $\mu$ CT and  $\mu$ CT datasets. From the  $\mu$ CT data the tissue mineral density (TMD) and local variance in the grey-level values were analyzed. The local variance analysis was applied in 3D by calculating the 2D GLCM's through the stacks in 7 different rotational angles and summing the GLCMs. From the summed GLCM, GLCM contrast (describes the local variance of the neighboring grey-level values) was calculated. From the SR $\mu$ CT data, osteocyte cellularity analyses were performed with the CTAn software (v.1.17.7.2, Bruker microCT). Correlations between the calculated GLCM contrast, TMD, and osteocyte cellularity were done with Pearson's  $r$  test. Correlation between contrast and OARSI grade were evaluated with Spearman's rho test.

**Results:** GLCM contrast increased with cellularity ( $R=0.518$ ,  $p=0.007$ ) and OARSI grade ( $\rho=0.585$ ,  $p=0.001$ ). No significant association between GLCM contrast and the TMD (see Figure 1) was found.

**Conclusions:** As hypothesized, local grey-level variance in 3D from the desktop  $\mu$ CT was associated with the osteocyte cellularity determined

from SR $\mu$ CT images. Even though no significant association between the TMD and the GLCM features was found, significant correlation with OARSI grade indicated that local variability in the TMD was also present. The method presented here could indirectly allow analysis of osteocyte cellularity and local variability in TMD, which both are important descriptors of subchondral bone remodeling, from the conventional desktop  $\mu$ CT systems that are widely available.

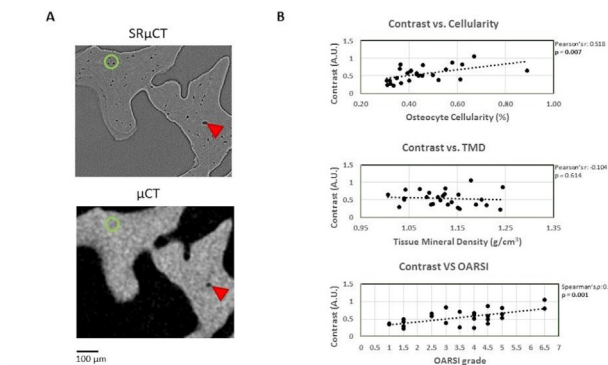


**Figure 1.** A) Slices from small areas of co-registered  $\mu$ CT and SR $\mu$ CT VOLS. Red arrow shows vascular channels which were not included in the analyses. Green circle shows visible osteocytes (3 cells) in SR $\mu$ CT and corresponding area from  $\mu$ CT from which osteocyte cellularity cannot be analyzed with standard analysis methods. Scale bar shown on the bottom left corner. B) Correlations between GLCM contrast (describes local grey-level variance) and with osteocyte cellularity, tissue mineral density (TMD), and OARSI histological grading. Correlation coefficients and statistical significances presented on the right.

## 158

### OVARECTOMY INDUCED BONE LOSS IS ANTAGONIZED BY PULSED ELECTROMAGNETIC FIELDS (PEMFs) AND TNF- $\alpha$ AND IL-6 GENE KNOCKOUTS IN A SIMILAR MECHANISM

S. Zhu<sup>†,‡</sup>, H. He<sup>‡</sup>, H. Wang<sup>‡</sup>, C. Gao<sup>‡,§</sup>, Q. Wang<sup>‡</sup>, D. Wang<sup>||</sup>, Q. Wei<sup>¶</sup>, X. Yu<sup>¶</sup>, C. He<sup>‡,§</sup>. <sup>†</sup>Arthritis Res. Canada, Univ. of British Columbia, Richmond, BC, Canada; <sup>‡</sup>Rehabilitation Ctr., West China Hosp., Sichuan Univ., Chengdu, China; <sup>§</sup>Inst. for Disaster Management and Reconstruction, Sichuan Univ.-The Hong Kong Polytechnic Univ., Chengdu, China; <sup>||</sup>Sch. of Aeronautics and Astronautics, Sichuan Univ., Chengdu, China; <sup>¶</sup>Lab. of Endocrinology and Metabolism, Dept. of Endocrinology, Natl. Key Lab. of Biotherapy/Collaborative Innovation Ctr. of Biotherapy and Cancer Ctr., West China Hosp., Sichuan Univ., Chengdu, China

**Purpose:** Pulsed electromagnetic fields (PEMFs), as a safe and non-invasive method, could promote in vivo and vitro osteogenesis. However, the effect and underlying mechanisms of PEMFs on postmenopausal osteoporosis remain poorly understood. The present study is designed to investigate the effect of PEMFs on osteoporotic bone microarchitecture and abnormal bone metabolism together with its potential molecular mechanisms in ovariectomized (OVX) mice with different gene background.

**Methods:** Twenty 12-week Female wild-type (WT), *TNF $\alpha$*  knockout (*TNF $\alpha$ <sup>-/-</sup>*) or *IL6* knockout (*IL6<sup>-/-</sup>*) mice, respectively, were sham-operated (SHAM) or subjected to OVX. After OVX, WT mice were equally assigned to the non-treatment and PEMFs groups. Mice in PEMFs group were subjected to daily 1-hour PEMFs exposure with 8 Hz, 3.8 mT (peak value). Then all mice were euthanized after 4 weeks. Bone mass and skeletal microarchitecture were determined using micro-CT. Bone metabolism was assessed by histological analysis, serum analyses and qRT-PCR.

**Results:** OVX significantly increased the body weight only in WT mice without PEMFs treatment and decreased the uterine weight in all groups. The high bone turnover induced by OVX was largely repaired by *TNF $\alpha$*  and *IL6* gene knockout and partially inhibited by PEMFs exposure. The ratio of femoral trabecular bone volume to tissue volume (BV/TV), trabecular number (Tb.N) and trabecular thickness (Tb.Th) were significantly decreased in WT mice subjected to OVX, but increased in PEMFs group (0.89, 0.61, 0.27-fold respectively), *TNF $\alpha$ <sup>-/-</sup>* mice (1.54, 1.29, 0.30-fold respectively) and *IL6<sup>-/-</sup>* mice (1.18, 0.75, 0.24-fold respectively). Furthermore, no difference in Micro-CT data analysis was found between PEMFs group and gene knockouts mice after OVX, although 38.5% and 45.1%, respectively, increase in BV/TV and Tb.N were observed in *TNF $\alpha$ <sup>-/-</sup>* mice when compared to the PEMFs group. The trends was further confirmed by bone histological analysis (H&E staining). OVX failed to increase the number and size of TRAP-positive cells in PEMFs group and gene knockouts mice, although the phenomenon was more